Progress In Electromagnetics Research C, Vol. 75, 87–97, 2017

Sensitivity Modeling of a Strain-Sensing Antenna

Lan Chen[1], Tao Geng[1], Guochun Wan[2], Ling Yi Tang[2], and Mei Song Tong[2, *]

Abstract—A quarter-wavelength folded patch antenna is adopted as the passive wireless strain sensor for structural health monitoring (SHM) of bridges. It can be used for continuous surveillance and damage detection. According to theoretical formulations, strain simulation and experiments, it is found that a good linearity relationship can be achieved between normalized resonance frequency shift and the strain both in longitudinal and transverse directions. And the sensing sensitivity in longitudinal strain is better than that in transverse strain. Through conducting tensile experiments, we find that many factors can influence the strain sensitivity. To address this fundamental issue in antenna sensors for strain sensing, a new strain sensitivity experiment is proposed to take the influence of strain transfer ratio change under strain. The linear relationship of strain transfer ratio and deformation is obtained by sensitivity experiment. The corrected sensitivity in longitudinal and transverse strains is calculated based on the linearity. Furthermore, the Possion effect is taken into consideration to explain the opposite effects of experimental and simulated sensitivities in transverse strain.

1. INTRODUCTION

Metallic dampers in a bridge's structure have the effect of shock absorption when earthquake happens, and it will suffer from a certain degree of damage and destruction. Structural health monitoring (SHM) on bridge's structure is the process of continuous surveillance and damage detection in order to facilitate maintenance and retrofitting decisions [1].

Lots of sensing techniques are used in the SHM. Traditional monitoring methods, such as metal foil strain gauges or fiber optic sensors, generally require cabled installation of the sensor and associated data acquisition system [2–5]. To eliminate the high cabling cost for large structures, wireless sensing devices have been developed for digitizing and transmitting sensor data [6, 7]. But these devices usually require batteries or energy harvesters for power supply. Passive wireless strain sensing through analog mechanisms was proposed to reduce the complexity of the wireless nodes.

Passive wireless antenna sensors have been developed to overcome those problems in recent years and have been applied in strain measurement. In this paper, the probability that a folded patch antenna is used as strain sensor is studied. It is known that electromagnetic backscattering techniques have been exploited for wireless strain sensing [8]. Since the electromagnetic resonance frequency of an antenna is related to the antenna's physical dimension, the resonance frequency changes when the antenna is subject to a strain [9, 10]. With mathematical deduction, it is found that there is a good linear relationship between simulated resonance frequency shift and the strain. After bonding or embedding the antenna to a structure, this relationship between resonance frequency and strain can be used for strain measurement. According to the various engineering demands involved in SHM, three basic goals are proposed for designing a passive wireless antenna sensor. Firstly, there is a good linear relationship

Received 13 March 2017, Accepted 27 May 2017, Scheduled 17 June 2017

* Corresponding author: Mei Song Tong (mstong@tongji.edu.cn).

[1] School of Electrical and Electronic Engineering, Shanghai Institute of Technology, Shanghai, China. [2] Department of Electronic Science and Technology, Tongji University, Shanghai, China.

between resonance frequency shift and the strain. Secondly, the sensing sensitivity in longitudinal strain is better than that in transverse strain. Lastly, there is a much smaller power reflection coefficient on resonance frequency.

The paper is organized as follows. Section 2 describes strain sensing mechanism of the folded patch antenna sensor and proposes the mechanics-electromagnetics coupled simulation model. Section 3 presents experimental strain sensing results of the antenna sensor. Section 4 takes into account the transfer strain ratio and Possion effect to do further research on sensitivity of longitudinal and transverse strain. Section 5 provides a summary and discussion.

2. SENSING MECHANISM AND MECHANICS-ELECTROMAGNETICS COUPLED SIMULATION

In this section, the probability that the folded patch antenna is used as a strain sensor is studied. To reduce the size of the sensors, a quarter-wavelength folded patch antenna is adopted. The quarter-wavelength folded patch antenna has the same Q as full-sized patch antenna. Its top copper and ground plane are connected with a metallic via hole. The width of the top copper $L_{1/4}$ can be calculated by the following equation [11].

$$W = \frac{C}{2f}\left(\frac{\varepsilon_{re}+1}{2}\right)^{-\frac{1}{2}} \tag{1}$$

The length of top copper $L_{1/4}$ can be calculated by the following equation.

$$L_{1/4} = \frac{\lambda}{4\sqrt{\varepsilon}_{re}} - 2\Delta L_{oc} \tag{2}$$

The effective dielectric constant of the substrate ε_{re} is related to the relative dielectric constant of the substrate ε_r, the physical width of the top copper cladding W and the antenna substrate thickness h:

$$\varepsilon_{re} = \frac{\varepsilon_r+1}{2} + \frac{\varepsilon_r-1}{2\sqrt{1+10h/W}} \tag{3}$$

For a quarter-wavelength folded patch antenna, the resonance frequency of the antenna under a strain, f_{res}, can be approximated with the following equation.

$$f_{res} = \frac{c}{4\sqrt{\varepsilon_{re}}}\frac{1}{L+2\Delta L_{oc}} \tag{4}$$

where c is the speed of light, L the physical length of the top copper cladding, ε_{re} the effective dielectric constant of the substrate, and ΔL_{oc} the additional electrical length compensation determined by the substrate's width-to-thickness dimension and the dielectric constant. The additional electrical length compensation ΔL_{oc} is related to effective dielectric constant of the substrate, the antenna's substrate thickness and the physical width of the top copper cladding [12].

$$\Delta L_{oc} = 0.412h\frac{(\varepsilon_{re}+0.3)\left(\frac{W}{h}+0.264\right)}{(\varepsilon_{re}-0.258)\left(\frac{W}{h}+0.813\right)} \tag{5}$$

Assuming that the longitudinal strain ε_L increases, the resonance frequency will shift. In engineering, a strain is usually defined as the relative change of length when an object deforms:

$$\varepsilon_L = \frac{L-L_0}{L_0} \tag{6}$$

The unit of strain is dimensionless, which is usually denoted as $\mu\varepsilon$ (microstrain). One $\mu\varepsilon$ means 1×10^{-6} or 1 ppm (parts per million) relative change in length. Assuming that the strain $\mu\varepsilon$ increases, the antenna's substrate thickness and the physical width of the top copper cladding will change, i.e.

$$\begin{aligned} W &= (1-\nu_p\varepsilon_L)W_0 \\ h &= (1-\nu_s\varepsilon_L)h_0 \end{aligned} \tag{7}$$

where ν is the Poisson's ratio, which is the absolute ratio between transverse strain and longitudinal strain of the antenna when a force is applied longitudinally, ν_p the Poisson's ratio of top copper, and ν_s the Poisson's ratio of top copper, dielectric substrate. Assuming that ν_p and ν_s are the same or similar, the ratio W/h will not change with increasing strain. Therefore, the relative dielectric constant of the substrate ε_{re} is independent of strain, and there is direct proportion relationship between the additional electrical length compensation ΔL_{oc} and the antenna substrate thickness. According to Equation (1), the resonance frequency of the antenna under strain can be redefined in the following equation.

$$f_{res} = \frac{c}{4\sqrt{\varepsilon}_{re}} \frac{1}{L + 2\Delta I_{oc}} = \frac{C_1}{L + C_2 h} \tag{8}$$

where $C_1 = \frac{c}{4\sqrt{\varepsilon_{re}}}, C_2 = 0.824 \frac{(\varepsilon_{re}+0.3)(\frac{W}{h}+0.264)}{(\varepsilon_{re}-0.258)(\frac{W}{h}+0.813)}$. If strain ε_L increases, the resonance frequency is estimated in the following equation:

$$f_{res}(\varepsilon_L) = \frac{C_1}{L(1+\varepsilon_L) + C_2 h(1-\nu\varepsilon_L)} \tag{9}$$

With Equations (8) and (9), Δf_L can be approximately derived by following equation.

$$\begin{aligned} \varepsilon_L &= -\frac{L + C_2}{L - \nu C_2 h} \frac{f_{res}(\varepsilon_L) - f_{res}}{f_{res}} = -\frac{L + C_2}{L - \nu C_2 h} \Delta f_L \\ \rightarrow \Delta f_L &= -\frac{L - \nu C_2 h}{L + C_2} \varepsilon_L = K_1 \varepsilon_L \end{aligned} \tag{10}$$

where

$$f_{res}(\varepsilon_L) = -\frac{L - \nu C_2 h}{L + C_2} f_{res} \varepsilon_L + f_{res} \approx K_2 \varepsilon_L + f_{res} \tag{11}$$

It is found that $K_2 \approx -f_{res}$. The sensing sensitivity of strain sensor is related with its working frequency and the material of dielectric substrate. From Equation (11), it is found that the coefficient K_2 is related with not only Poisson's ratio of antenna, but also its physical shape. Assuming that transverse strain ε_W increases, the resonance frequency will shift. In engineering, strain is usually defined as relative change of width when an object deforms:

$$\varepsilon_W = -\frac{W - W_0}{W_0} \tag{12}$$

Assuming that if strain ε_H increases, the antenna substrate thickness and the physical length of the top copper cladding will change. When force applied transversely, assume that Poisson's ratio ν_W is the same or similar in length and height.

$$\begin{aligned} L &= (1 - \nu_W \varepsilon_W) L_0 \\ h &= (1 - \nu_W \varepsilon_W) h_0 \end{aligned} \tag{13}$$

Assume that the relative dielectric constant of the substrate ε_r is independent from strain, and when strain is less than $50000\,\mu\varepsilon$, the ratio W/h will not change. So the effective dielectric constant of the substrate $\varepsilon_r e$ and coefficient C_2 remain unchanged. If strain ε_W increases, the resonance frequency can be estimated in the following equation:

$$f_{res}(\varepsilon_L) = -\frac{C_1}{L(1 - \nu_w \varepsilon_w) + C_2 h(1 + \varepsilon_w)} \tag{14}$$

With Equations (8) and (14), Δf_w can be approximately derived by the following equation.

$$\begin{aligned} \varepsilon_W &= -\frac{\nu_W L - C_2 h}{L + C_2 h} \frac{f_{res}(\varepsilon_W) - f_{res}}{f_{res}} = -\frac{\nu_W L - C_2 h}{L + C_2 h} \Delta f_W \\ \rightarrow \Delta f_W &= -\frac{L + C_2 h}{\nu_W (L - C_2 h/\nu_W)} \varepsilon_W = K_3 \varepsilon_W \end{aligned} \tag{15}$$

$$f_{res}(\varepsilon_W) = -\frac{\nu_W L - C_2 h}{L + C_2 h} f_{res} \varepsilon_W + f_{res} = K_4 \varepsilon_W + f_{res} \tag{16}$$

where $K_3 = -\frac{\nu_W L - C_2 h}{L + C_2 h} f_{res} = -(\nu_W - \frac{(1+\nu_W)h}{L+C_2 h} f_{res})$. From Equation (15), it is found that the coefficient K_3 is related with not only Poisson's ratio of antenna, but also its physical shape. If transverse strain increases, the resonance frequency decreases due to Poisson effect, while the change is obviously smaller than the former one. So the relationship between resonance frequency and longitudinal strain can be used for strain measurement.

We have verified the probability that folded patch antenna can be applied as strain sensor. HFSS has the great function of electromagnetic model simulation and calculation thus use HFSS to establish the model of folded patch antenna with quarter-wavelength. From Equation (4), it is found that the resonance frequency is related to antenna's size. The bigger the antenna sensor is, the higher the resonance frequency is and the better the sensing sensitivity will be. In order to simplify the experiment, the antenna is fed by a microstrip line. According to Equations (1), (2), the model is built as in Figure 1.

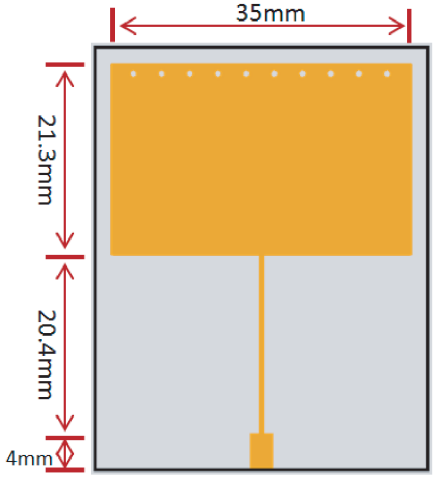

Figure 1. The model of folded patch antenna with 1/4 wavelength.

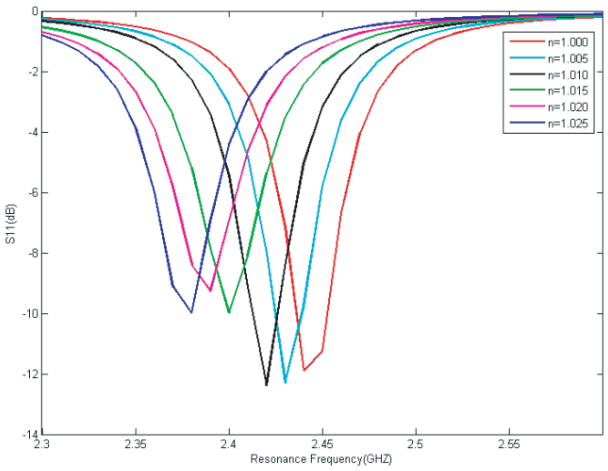

Figure 2. Normalized resonance frequency change in longitudinal strain.

The material of dielectric substrate is $RT5880$ in which dielectric constant is 2.2 under zero-strain. The substrate thickness is $H = 0.51$ mm. The planar dimensions of the copper antenna are $L_0 \times W_0 = 21.3 \times 35$ mm. The planar dimensions of impedance matching line are $L_1 \times W_1 = 20.4 \times 0.3$ mm. The planar dimensions of port are $L_2 \times W_2 = 4 \times 2.5$ mm. The diameter of via hole is 0.5 mm. The final simulated resonance frequency is 2.44 GHz. Theoretical calculation and modeling of the folded patch antenna with 1/4 wavelength have already been finished. But in order to verify the expected result, that simulated resonance frequency shift and the strain form a good linear relationship, further simulation is needed. In order to simplify the simulation, two assumptions are proposed. First, ignoring the deformation and the impact on the relative dielectric constant; second, assuming that the dielectric substrate, top copper and ground plane have the same strain during deformation process. The proportion of strain n means $(L + \Delta_L)/L$. Firstly, we apply tensile simulation on the strain sensing performance, whose strain range is from $5000\mu\varepsilon$ to $25000\mu\varepsilon$ (the range of n is from 1.005 to 1.025). The tensile load is configured so that an approximately 5000 increment is achieved at each step. Figure 2 shows that power reflection coefficient under different strain changes is less than -10 db. The attenuation is easy to be detected, and it is one of the conditions to be strain sensor.

Then, tensile simulation is conducted on the sensing performance of transverse strain. The strain range is from $5000\mu\varepsilon$ to $25000\mu\varepsilon$ (the range of n is from 1.005 to 1.025). The tensile load is configured so that an approximately $5000\mu\varepsilon$ increment is achieved at each step. Figure 3 shows that power reflection coefficient under different strain changes is less than -10 db.

The fitting curve of relationship between resonance frequency and strain is obtained from the simulation results. Figure 4 shows the sensing sensitivity in longitudinal strain and transverse strain.

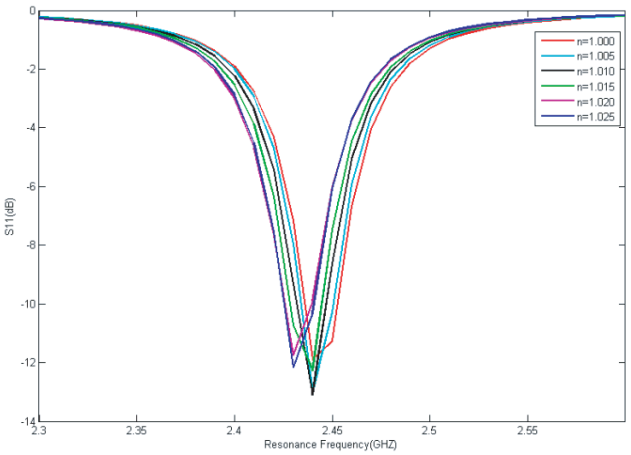

Figure 3. Normalized resonance frequency change in transverse strain.

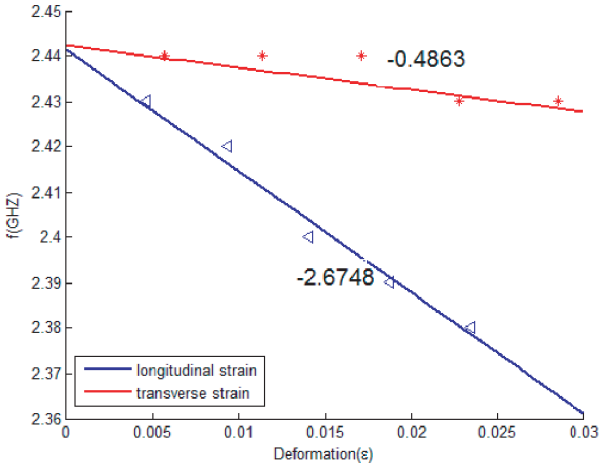

Figure 4. Sensing sensitivity in longitudinal strain and transverse strain.

Sensing relationship in longitudinal strain and transverse strain is shown as bellow.

$$\begin{aligned} f_L &= -2.6748\varepsilon_L + 2.4414 \\ f_W &= -0.4843\varepsilon_W + 2.4424 \end{aligned} \tag{17}$$

Equation (17) shows that sensing sensitivity in longitudinal strain is -2.6748, which is 5 bigger than the sensitivity in transverse strain. So the relationship between resonance frequency and longitudinal strain can be used for strain measurement.

3. SENSOR SETUP AND EXPERIMENTS

After optimization through simulation, the antenna sensor design is finalized and ready for fabrication. The antenna sensor prototype is built by standard PCB fabrication on a $RT5880$ substrate. The original resonance frequency of the folded patch antenna is 2.5205 GHz, and the reflection coefficient is -16 db. Figure 5 shows a photo of a fabricated folded patch antenna in longitudinal and transverse directions. The antenna sensors are attached on the surface of aluminum specimen by glue. The resonance frequency of the antenna without strain is 2.5118 GHz, and the reflection coefficient is -18.6 db. The difference of resonance frequency is attributed to the aluminum specimen and the deformation caused by attaching. However, this paper studies the sensitivity of antenna sensor, and the sensitivity represents the resonance frequency shift during strain. So, to simplify the sensitivity modeling, the influence of aluminum specimen is ignored here. The aluminum specimen is made into a special shape, which is easy to be clamped, and its thickness is 4 mm.

Figure 6 shows the experimental setup for the tensile test. The resonator is installed along the side of an aluminum specimen. The S_{11} coefficient of the resonator is measured by a vector network analyzer (VNA). The tensile testing machine is configured so that a strain increment is approximately achieved at each loading step. Dynamometer measures the force applied on the specimen by the tensile testing machine. The real strain can be calculated with the following equation.

$$\varepsilon = \frac{F}{E \times A} \tag{18}$$

where, ε is the strain value of aluminum specimen, E the elasticity modulus of aluminum specimen, A the cross-sectional area of aluminum specimen, and F the force applied on specimen.

Two experiments are conducted in order to obtain the performance in longitudinal and transverse strains. $2KN$ is tried to be applied on specimen in each step, until the loading is up to about $12KN$. Finally, 7 sets of data are obtained, including the original data and 6 steps. But the

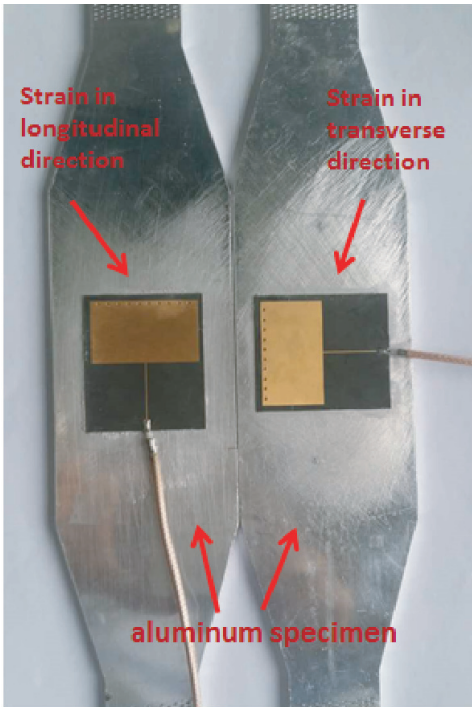

Figure 5. Folded patch antenna bonded in longitudinal and transverse direction.

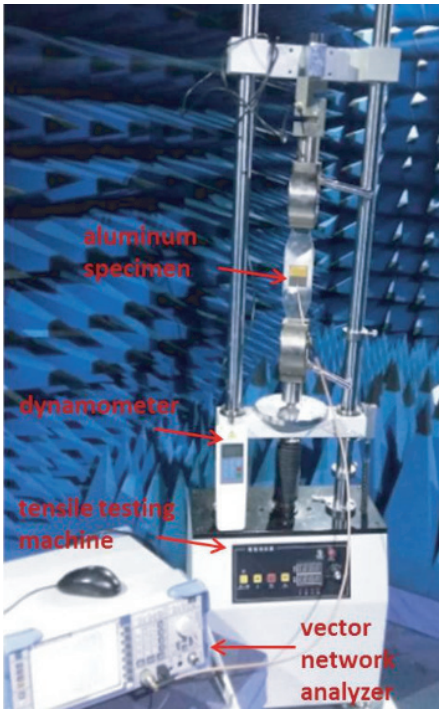

Figure 6. Experimental setup for the tensile test.

tensile testing machine cannot supply uniform and accurate tension, and the actual tension of each loading step is measured by dynamometer respectively. During experiment of longitudinal strain, the antenna sensor is bonded as the left one in Figure 5. The measured tension is $0KN, 2.12KN, 6.04KN, 7.88KN, 10.08KN, 12.20KN$. According to Equation (17), the calculated deformation is $0\mu\varepsilon, 129\mu\varepsilon, 255\mu\varepsilon, 363\mu\varepsilon, 477\mu\varepsilon, 609\mu\varepsilon, 737\mu\varepsilon$. Too much loading should be avoided because it will lead to specimen cracking, and the measurement is inaccurate if specimen gets cracked. The resonance frequency of each loading step will be read through vector network analyzer. Figure 6 shows the resonance frequency shift in each loading step during longitudinal strain.

Figure 7 shows that power reflection coefficient in different strain changes is less than -10 db. There is an obvious frequency shift on each strain change. Then, experiment of transverse strain is conducted. The antenna sensor is bonded as the right one in Figure 5. The actual tension is $0KN, 2.44KN, 4.28KN, 6.48KN, 8.47KN, 10.32KN, 12.02KN$. According to Equation (17), the calculated deformation is $0\mu\varepsilon, 147\mu\varepsilon, 258\mu\varepsilon, 393\mu\varepsilon, 512\mu\varepsilon, 625\mu\varepsilon, 727\mu\varepsilon$. Finally, the relationship between frequency drift rate and deformation is obtained through linear regression. Figure 8 shows the fitting curve of these two experiments.

Sensing relationship in longitudinal strain and transverse strain is shown as bellow.

$$\begin{aligned} \Delta f_L &= -0.6114\varepsilon_L \\ \Delta f_W &= -0.2536\varepsilon_W \end{aligned} \tag{19}$$

To compare experimental results with simulated ones, the fitting curve of simulation in longitudinal and transverse strains is redrawn as in Figure 9.

Figure 9 shows simulated curve between frequency drift rate and deformation through linear regression. The slope of experiment is -0.6114, and that of the simulation is -1.0962 in longitudinal strain. Moreover, the slope of experiment is 0.2564, and that of simulation is -1.0962 in transverse strain. There is an obvious discrepancy between the measured and simulated normalized strain sensitivities both in longitudinal and transverse strains.

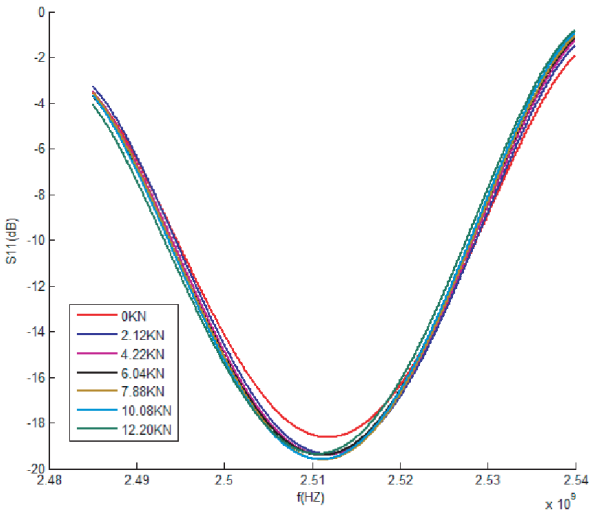

Figure 7. Resonance frequency shift during longitudinal strain.

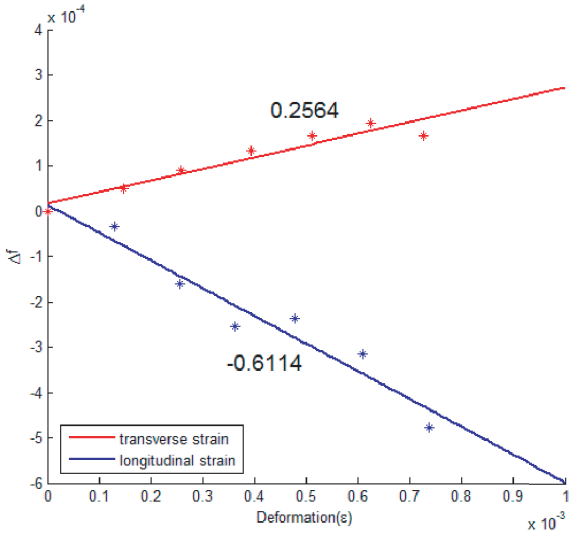

Figure 8. Fitting curve of experiment in longitudinal and transverse strain.

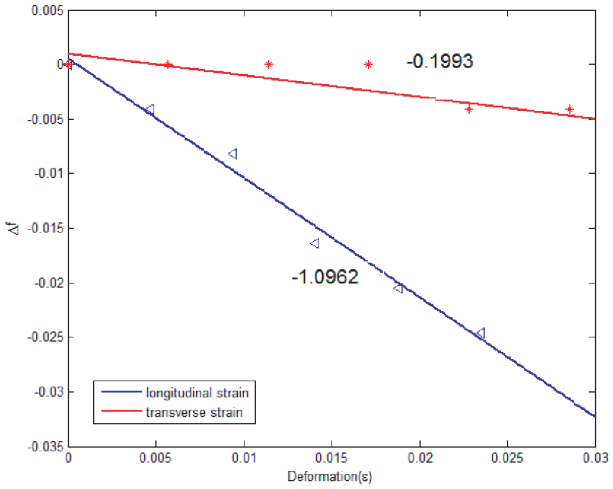

Figure 9. Fitting curve of simulation in longitudinal and transverse strains.

4. ANALYSIS OF EXPERIMENT RESULTS

The difference between the experimental and simulated data in longitudinal strain is caused by many reasons. One of them is that the substrate expansion and the changes in the material's dielectric properties under strain, which is not considered in the simulation model. Contrary to ideal materials, small voids always exist in practical substrate materials [10]. The distortion of the voids under strain affects the dielectric constant of the substrate, although very limited information is available from the manufacturer datasheet for the substrate. But the constant change of the substrate caused by tiny deformation is so small that accurate change cannot be detected through simple experiment. Another reason could be the strain transfer ratio between the top copper cladding of the sensor and aluminum specimen. During the measurements, the sensor is attached to the structural surface by superglue. The strain experienced by the top copper cladding is smaller than the strain on the bottom copper ground

plane and the structural surface. The strain transfer ratio is defined as bellow:

$$\eta = \frac{\varepsilon_t}{\varepsilon_s} \tag{20}$$

where η is the strain transfer ratio, ε_t the tensile strain experienced on the top copper cladding, and ε_s the actual strain on the specimen's surface. Under a certain circumstance that there is a firm bonding between the specimen and the bottom copper cladding of the antenna sensor, ε_s is also the tensile strain at the bottom copper cladding. In order to quantify the strain transfer ratio η, mechanical strain transfer experiments can be conducted to determine the ratio at different strain levels.

Figure 10 shows the mechanical strain transfer experiments. Two resistive strain gauges were attached on the surface of top copper cladding, and the other two resistive strain gauges were attached on the surface of aluminum specimen. Then, we conducted 5 levels of mechanical strain and record the deformation. The deformations on different positions of specimen are shown in Table 1.

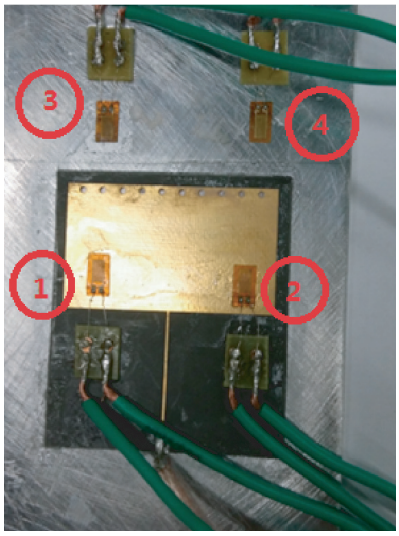

Figure 10. Experiment of strain transfer ratio.

Table 1. Deformation on different position.

	Position 1	Position 2	Position 3	Position 4
Level 0	0	0	0	0
Level 1	109	106	118	111
Level 2	203	165	209	200
Level 3	312	259	342	344
Level 4	387	320	441	451
Level 5	498	417	586	600

We found that strain transfer ratio is different when strain level is different. Linear regression was used to model the data, and the linearity of strain transfer ratio and deformation is shown in Figure 11.

So the relationship can be shown in the following equation.

$$\eta = -397.2987\varepsilon + 0.9850 \tag{21}$$

According to strain transfer ratio described in the equation, we calculated the actual deformation of the antenna sensor. The calculated deformation is $0\mu\varepsilon, 129\mu\varepsilon, 255\mu\varepsilon, 363\mu\varepsilon, 477\mu\varepsilon, 609\mu\varepsilon, 737\mu\varepsilon$. The corrected fitting curves of experiment in longitudinal and transverse strains are shown in Figure 12.

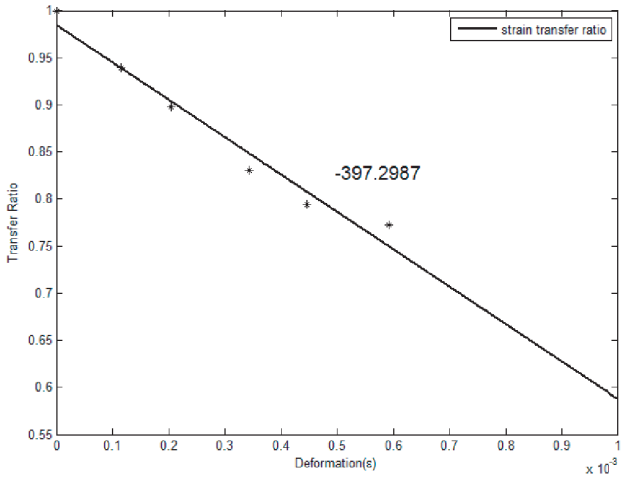

Figure 11. The linearity of strain transfer ratio and deformation.

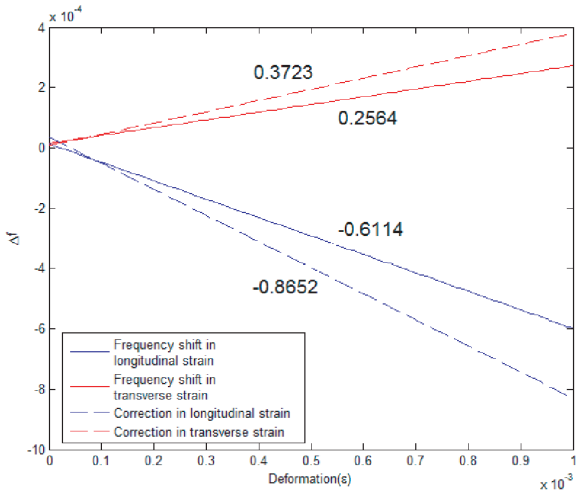

Figure 12. Correction of experimental results.

The slope of corrected curve in longitudinal strain is −0.8652, close to the expected value. However, the discrepancy between the measured and simulated normalized strain sensitivities in transverse strain becomes worse. The simulated sensitivity is −0.1993, and corrected experimental sensitivity is 0.3723, so they show the opposite effects. Simulated sensitivity shows that when transverse strain is happening, the frequency gets lower. However, the corrected experimental sensitivity shows that when transverse strain is happening, the frequency gets higher. The main reason may be due to Poisson's effect during the transverse strain. In fact, during the deformation, because of the existence of Poisson effect, the length and width of the antenna will influence each other. When longitudinal strain happens, antenna will contract in transverse direction. Longitudinal contraction will also happen when transverse strain happens.

In the process of specimen stretching, the stress distribution on the surface of the aluminum plate contributes to antenna's deformation. Assuming that antenna is bonded firmly and can transfer strain well, the antenna of Poisson's ratio should be consistent with the aluminum specimen, 3.3. So, during the longitudinal deformation, the resonance frequency deviation is not only related to the longitudinal deformation, but also related to the transverse deformation caused by Poisson effect. According to Equations (10) and (15), the relationship between resonance frequency deviation and strain can be corrected as bellow.

$$\begin{aligned} \Delta f_L &= K_L \varepsilon_L - K_W \nu_A \varepsilon_L + K_0 \\ \Delta f_W &= K_W \varepsilon_W - K_L \nu_A \varepsilon_W + K_0 \end{aligned} \tag{22}$$

where Δf_L is the resonance frequency drift rate of longitudinal strain, Δf_W the resonance frequency drift rate of transverse strain, ε_L the longitudinal strain, ε_W the transverse strain, ν the Possions ratio of aluminum specimen, K_L sensitivity of resonance frequency drift rate and longitudinal strain, K_W the sensitivity of resonance frequency drift rate and transverse strain, and K_0 the other factors which influence the resonance frequency. Assuming that K_0 can be neglected, passion effect will be taken into consideration. Relationship between resonance frequency drift rate and strain will be redefined as shown in Figure 13.

According to Figure 13, the simulated sensitivity of transverse strain with passion effect is 0.1661, which has approximately the same trend as the experimental sensitivity.

Another possible explanation may be relevant to the structure of the resonator presented. The resonator includes not only the center transmission line, but also one feeding line for the measurement at the port. Under mechanical loading, the feeding line also deforms and thus contributes to the overall resonance frequency change (in addition to the contribution from the dielectric constant change). This effect from the feeding line is difficult to quantify and may reduce the accuracy of the dielectric constant characterization.

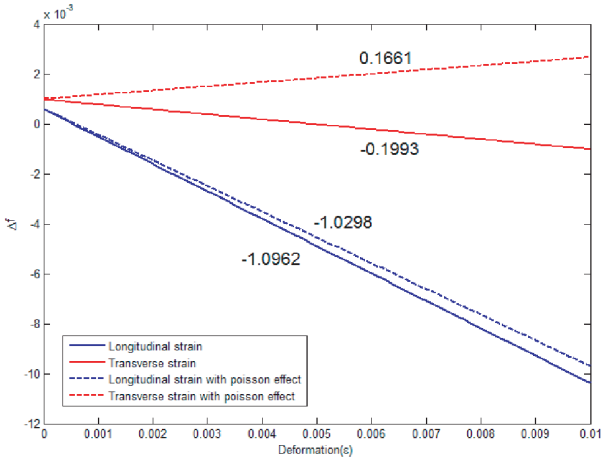

Figure 13. Sensitivity with passion effect.

5. CONCLUSION

In this paper, a type of folded patch antenna, with 1/4 wavelength and via holes is proposed for strain measurement. Firstly, it is proved that folded patch antenna can be used as strain sensor, and an electromagnetics model is built through applying HFSS. According to theoretical formulations and strain simulation, we can conclude as follows. There is a good linear relationship between the normalized resonance frequency shift and the strain. The bigger the antenna sensor is, the higher the resonance frequency is and the better sensing sensitivity is. The sensing sensitivity in longitudinal strain is better than that of the transverse strain. Tensile tests are conducted in order to verify these conclusions. From tensile tests, many factors are found to have an impact on strain sensitivity. To address this fundamental issue in antenna sensors for strain sensing, a new strain sensitivity experiment is proposed for considering the influence of strain transfer ratio change under strain. Furthermore, the Possion effect is taken into account to explain the opposite effects of experimental and simulated sensitivities in transverse strain. In conclusion, we should take the size and sensing sensitivity into comprehensive consideration, if we use a folded patch antenna as the strain sensor.

REFERENCES

1. Sohn, H., et al., "A review of structural health monitoring literature: 1996–2001," *Tech. Rep. LA-13976-MS*, Los Alamos Nat. Lab., Los Alamos, NM, USA, 2003.
2. Michie, W. C., B. Culshaw, S. S. J. Roberts, and R. Davidson, "Fiber optic technique for simultaneous measurement of strain and temperature variations in composite materials," *Proc. SPIE*, Vol. 1588, Boston, MA, USA, Dec. 1991.
3. Lynch, J. P. and K. J. Loh, "A summary review of wireless sensors and sensor networks for structural health monitoring," *Shock Vib Digest*, Vol. 38, 91–130, 2006.
4. Mohammad, I., V. Gowda, H. Zhai, et al, "Detecting crack orientation using patch antenna sensors," *Meas. Sci. Technol.*, Vol. 23, 015102, 2012, doi:10.1088/0957-0233/23/1/015102.
5. Murray, W. M. and W. R. Miller, *The Bonded Electrical Resistance Strain Gage: An Introduction*, Oxford Univ. Press, New York, NY, USA, 1992.
6. Liu, L. and F. G. Yuan, "Wireless sensors with dual-controller architecture for active diagnosis in structural health monitoring," *Smart Mater. Struct.*, Vol. 17, No. 2, 025016, Apr. 2008.
7. Kurata, N., B. F. Spencer, and M. Ruiz-Sandoval, "Risk monitoring of buildings with wireless sensor networks," *Struct. Control Health Monitor.*, Vol. 12, Nos. 3–4, 315–327, Jul./Dec. 2005.

8. Thai, T. T., G. R. DeJean, and M. M. Tentzeris, "A novel front-end radio frequency pressure transducer based on a dual-band resonator for wireless sensing," *IEEE MTT-S International Microwave Symposium Digest, 2009, MTT'09*, 1701–1704, IEEE, Boston, 2009.
9. Lee, H., G. Shaker, V. Lakafosis, et al., "Antenna-based 'smart skin' sensors for sustainable, wireless sensor networks," *2012 IEEE International Conference on Industrial Technology (ICIT)*, 189–193, IEEE, Athens, 2012.
10. Lee, H., K. Naishadham, M. M. Tentzeris, et al., "A novel highly-sensitive antenna-based 'smart skin' gas sensor utilizing carbon nanotubes and inkjet printing," *2011 IEEE International Symposium on Antennas and Propagation (APSURSI)*, 1593–1596, IEEE, Spokane, 2011.
11. Sohn, H., C. R. Farrar, F. M. Hemez, D. D. Shunk, D. W. Stinemates, and B. R. Nadler, "A review of structural health monitoring literature," 1996-2001 NM Report No. LA-13976-MS, Los Alamos National Laboratory.
12. Finkenzeller, K., *RFID Handbook*, 2nd edition, Wiley, New York, NY, USA, 2003.